

Parametric models of spatial birth-and-death processes
with a view to modelling linear dune fields

Jesper Møller and Michael Sørensen

Department of Theoretical Statistics

Institute of Mathematics

University of Aarhus

DK-8000 Århus C

Abstract

Statistical inference for parametric models of spatial birth-and-death processes is discussed in detail. In particular, a flexible and statistically tractable parametric class of such processes, defined on the real line, is presented. The suggested methods are illustrated by applying them to two sets of data given in the form of air photos from the Kalahari Desert.

Keywords: Delaunay tessellation; graphical methods; likelihood methods; linear dune fields; martingales; modelling and model control; nearest-neighbour birth-and-death processes on the real line; partial likelihood; spatial birth-and-death processes; Voronoi tessellation.

1. Introduction

Spatial birth-and-death processes have found frequent use in spatial statistics as a tool for simulating spatial point processes, which can be thought of as the equilibrium distribution towards which a spatial birth-and-death process converges, see Ripley (1977, 1981), Diggle (1983) and Baddeley and Møller (1989). In the present paper it is demonstrated that spatial birth-and-death processes are also very useful for modelling dynamical spatial processes. A flexible and statistically tractable parametric class of such processes, defined on the real line, is presented. The discussion is mainly focussed on modelling a particular phenomenon, namely linear dune fields, but the model presented is obviously applicable in many other contexts, and most of the methods proposed can be generalized straightforwardly to other birth-and-death process models. For general results on spatial birth-and-death processes, see Preston (1977), for processes on the real line in particular, see Holley and Stroock (1978).

Linear dune fields are described in Section 2. Here we also present two sets of data given in the form of air photos from the Kalahari Desert. Some necessary results on spatial birth-and-death processes on the real line are given in Section 3, where also our particular parametric sub-class is defined and some of its probabilistic properties are discussed. The proofs are given in Appendix 1. Likelihood functions and partial likelihood functions are derived in Section 4. The partial likelihood functions are also relevant to a semi-parametric model more general than

the model given in Section 3. It is proved that the maximum likelihood estimates exist with probability one, and conditions for the existence of the maximum partial likelihood estimates are formulated and discussed. Asymptotic properties of the estimators and of test statistics are discussed, but not rigorously proved, in Appendix 2. In Section 5 the air photo data on linear dune fields are analysed by means of the model presented in Section 3. In Section 6 methods, mostly graphical, for checking the consistency of our model with the data are proposed and applied to the dune data. Finally, extensions to higher dimensions are considered in Section 7.

2. Data on linear dune fields

The data to be modelled and analysed in the present paper consists of two air photos of different parts of a field of so-called vegetated linear dunes in the Kalahari Desert. A linear dune field is a large collection of parallel nearly linear sand dunes. The height of the dunes on the air photos is 2-15 meters, and their spacing is typically 200-500 meters. They can be several kilometers long.

The dunes are parallel to the direction of the prevailing wind. It is believed that dunes start in the lee of relatively densely vegetated sand patches behind which sand can accumulate. According to this theory the dune will, provided the sand supply is sufficient, grow in the downwind direction as a result of a positive feed-back mechanism between vegetation and sand deposition (Tsoar and Møller, 1986). Viewed in the downwind direction the dune field has a certain dynamics: As new dunes start, some of the old dunes that started further upwind will tend to end due to the limited sand supply. Most often they simply end, but on some occasions two dunes merge and continue downwind as one dune. The latter event is called a y-junction. It is assumed that in this way an equilibrium pattern develops in the wind direction. Presumably the new dunes do not start at completely random locations: There must be a higher tendency to dune development at places distant from other dunes where the sand supply is relatively large. It is the dynamics briefly outlined here that will be modelled by means of spatial birth-and-death processes in the

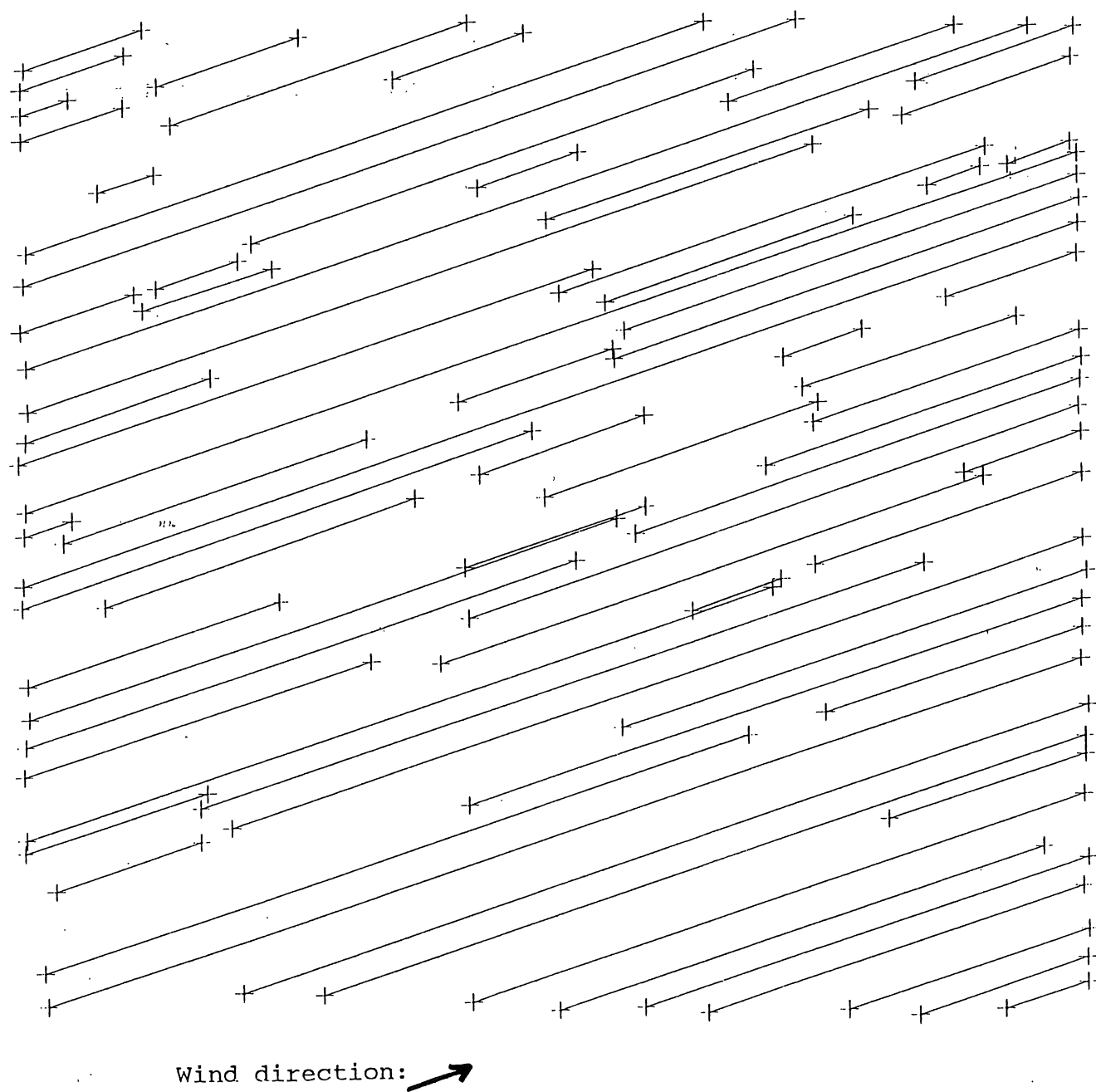


Figure 2.1. Parallel line segments fitted to the dunes on image 14a by linear regression.

next section.

The two air photos analysed in this paper were chosen because they contained only one or two y-junctions, so that this complication could be safely ignored. This was only done for the sake of simplicity of presentation. As discussed briefly in the next section, y-junctions can easily be built into our model. The birth-and-death process model assumes that the dunes are parallel line segments. The actual dune fields are, of course, not exactly like that, so as a preliminary step in the analysis of the data, parallel straight line segments were fitted to the dunes on each of the two air photos by usual linear regression. The two photos were originally called image 14a and image 15. We shall use these labels for future references. The estimated line segments for image 14a are given in Figure 2.1. The field of view in the figure is about 11 by 10.5 kilometers. The corresponding figure for image 15 looks similarly and is omitted here. Information, e.g. on dune spacing, needed in the statistical analysis was calculated from the position of the line segments.

3. Nearest-neighbour birth-and-death models on the real line

In this section we construct a stochastic model for the linear dune fields, cf. Section 2. The model is a nearest-neighbour birth-and-death process on the real line. Such processes are briefly reviewed in Subsection 3.1 and the model is presented in Subsection 3.2.

3.1. Birth-and-death processes on the real line

We shall consider finite birth-and-death processes on the real line, i.e. time homogeneous processes $\{x(t): t \geq 0\}$ where a state is a finite set of points contained in a bounded interval and where a transition is either the addition of a new point or the deletion of an existing point. More formally, let S be a bounded open interval on the real line and let, for each $n = 0, 1, 2, \dots$, Ω_n be the set of all point configurations $x = (x_1, \dots, x_n) \in S^n$ with $x_1 < \dots < x_n$. Especially, Ω_0 consists of the empty point configuration denoted by \emptyset . The state space of $x(t)$ is $\Omega = \bigcup_{n=0}^{\infty} \Omega_n$ and a transition from a state in Ω_n is either to Ω_{n+1} (a birth) or to Ω_{n-1} (a death). Let \mathcal{B} be the Borel σ -field on S , \mathcal{B}_n the corresponding σ -field on Ω_n , and \mathcal{F} the σ -field on Ω generated by $\{\mathcal{B}_n: n \geq 0\}$.

We shall henceforth assume that the process $\{x(t): t \geq 0\}$ is described, in a way indicated below, by two measurable and non-negative functions $b(x, \xi)$ and $d(x, \xi)$, $(x, \xi) \in \Omega \times S$, where

$b(x, \cdot)$ is Lebesgue integrable for all $x \in \Omega$ and where $d(0, \cdot) \equiv 0$. If $x = (x_1, \dots, x_n) \in \Omega$, write $x \setminus x_i$ for $(x_1, \dots, x_{i-1}, x_{i+1}, \dots, x_n)$. Further, let $x_0 < x_{n+1}$ denote the endpoints of the interval S . When $\xi \in S$ with $x_i < \xi < x_{i+1}$, we write $x \cup \xi$ for $(x_1, \dots, x_i, \xi, x_{i+1}, \dots, x_n)$. For $x \in \Omega$ and $A \in \mathcal{B}$ we define

$$B(x, A) = \int_A b(x, \xi) d\xi ,$$

$$\beta(x) = B(x, S) ,$$

$$\delta(x) = \begin{cases} \sum_{i=1}^n d(x \setminus x_i, x_i) & \text{if } x = (x_1, \dots, x_n) \text{ and } n > 0 , \\ 0 & \text{if } x = 0 , \end{cases}$$

$$\alpha(x) = \beta(x) + \delta(x) .$$

Finally, let $t_1 < t_2 < \dots$ denote the transition times for the process and set $t_0 = 0$.

Now we can define the spatial birth-and-death process in the following way: Given that $x(t_{j-1}) = x$ with $x = (x_1, \dots, x_n) \in \Omega_n$ and given the history of the process before time t_{j-1} , we require that

$$\begin{aligned} t_j - t_{j-1} & \text{ is exponentially distributed} \\ & \text{with mean } \alpha(x) , \end{aligned} \tag{3.1}$$

$$x(t_j) \in \Omega_{n+1} \text{ with probability } \beta(x)/\alpha(x) , \tag{3.2}$$

given that $x(t_j) \in \Omega_{n+1}$, i.e. that $x(t_j) = x(t_{j-1}) \cup \xi$, (3.3)
 then $\xi \in A$ with probability $B(x, A)/\beta(x)$,

given that $x(t_j) \in \Omega_{n-1}$, i.e. that $x(t_j) = x(t_{j-1}) \setminus \xi$, (3.4)
 then $\xi = x_i$ with probability $d(x \setminus x_i, x_i)/\delta(x)$.

Preston (1977) gives simple conditions for the unique existence of the above process and for its convergence to a limit distribution. Møller (1989) gives conditions ensuring a geometrically fast convergence. The limit distribution is the unique equilibrium distribution of the process. The density $f: \Omega \rightarrow [0, \infty]$ of this equilibrium distribution with respect to the measure μ on \mathcal{F} given by

$$\mu(F) = 1_F(0) + \sum_{n=1}^{\infty} \int_{x_0 < x_1} \dots \int_{x_n < x_{n+1}} 1_F((x_1, \dots, x_n)) dx_1 \dots dx_n$$

can be determined as follows when the process is time reversible. Assume that $d(\cdot, \cdot) > 0$ and define

$$\gamma(x, \xi) = b(x, \xi)/d(x, \xi) .$$

Furthermore, assume that a density f with respect to μ is defined inductively by

$$f(x \cup \xi) = \gamma(x, \xi) f(x) \quad (3.5)$$

and that

$$\int \beta(x) f(x) \mu(dx) < \infty. \quad (3.6)$$

The solution to (3.5) is well-defined if and only if a balance condition holds, viz.

$$\gamma(x \cup \xi, \eta) \gamma(x, \xi) = \gamma(x \cup \eta, \xi) \gamma(x, \eta). \quad (3.7)$$

Under the conditions imposed, the spatial birth-and-death process is time reversible and f is the equilibrium density, cf. Preston (1977, Theorem 8.1).

In this paper we shall concentrate on nearest-neighbour birth-and-death processes, i.e. processes where $b(x, \xi)$ and $d(x, \xi)$ depend only on ξ and its nearest left and right neighbours in x . Hence the equilibrium density (3.5) is seen to be Markov with respect to the sequential neighbour relation, cf. Baddeley and Møller (1989). We write $b(x_i, \xi, x_{i+1})$ for $b(x, \xi)$ and $d(x_i, \xi, x_{i+1})$ for $d(x, \xi)$ if $x_i < \xi < x_{i+1}$. Moreover, we define $H(x_i, x_{i+1}) = B(x, (x_i, x_{i+1}))$, which depends only on x_i and x_{i+1} . With this definition (3.3) naturally splits into the following two steps:

$$\begin{aligned} &\text{given that } x(t_j) \in \Omega_{n+1}, \text{ i.e. that } x(t_j) = \\ &x(t_{j-1}) \cup \xi, \text{ then } x_i < \xi < x_{i+1} \text{ with probability} \\ &H(x_i, x_{i+1}) / \beta(x), \quad i = 0, \dots, n, \end{aligned} \quad (3.8)$$

and

given that $x(t_j) = x(t_{j-1}) \cup \xi \in \Omega_{n+1}$ with (3.9)
 $x_i < \xi < x_{i+1}$, then ξ has a density on (x_i, x_{i+1})
 given by $h(\xi | x_i, x_{i+1}) = b(x_i, \xi, x_{i+1}) / H(x_i, x_{i+1})$,

where, in the first step,

$$\beta(x) = \sum_{i=0}^n H(x_i, x_{i+1}) . \quad (3.10)$$

3.2. Nearest-neighbour birth-and-death models for linear dune fields

For ease of presentation we shall only consider in detail a nearest-neighbour birth-and-death model for the linear dune fields in the case with no y-junctions. At the end of this section we briefly discuss the case where y-junctions are present.

Linear dunes are parallel to the direction of the prevailing wind, and they grow in this direction. It is therefore natural to define a 'time-axis' for a birth-and-death process parallel to the direction of the dunes and with time increasing in the prevailing wind direction. The state of the process $x(t)$ at 'time' t is the intersection points between the dunes and a bounded interval S of a line perpendicular to the wind direction that goes through the point t on the 'time axis'. The interval S should, of course, be large enough that the air photo under consideration is contained in $[0, \infty) \times S$. A birth and a

death for the process $\{x(t): t \geq 0\}$ corresponds respectively to the event that a new dune begins and the event that a dune ends. It is a very reasonable assumption that the birth or death of a dune is an event that is only affected by the presence of the two neighbouring dunes, so a nearest-neighbour birth-and-death process provides a good approximation to the dynamics of the dune field. Moreover, since there is only a limited supply of sand, the interaction between neighbouring dunes is expected to be a repulsion.

Let us now describe the model we propose. First consider the case where a birth occurs. In (3.8) and (3.9) we choose

$$H(x_i, x_{i+1})/\beta(x) = (x_{i+1} - x_i)^\gamma / \sum_{j=0}^n (x_{j+1} - x_j)^\gamma, \quad (3.11)$$

$$h(\xi | x_i, x_{i+1}) = \frac{\xi_i^{\alpha-1} (1-\xi_i)^{\beta-1}}{B(\alpha, \beta) (x_{i+1} - x_i)} \quad (3.12)$$

where $\gamma \in \mathbb{R}$, $\alpha, \beta > 0$, $B(\alpha, \beta)$ is the Beta function and

$$\xi_i = (\xi - x_i) / (x_{i+1} - x_i)$$

is the relative distance of the new dune to its nearest left neighbour dune. The choice of (3.11) and (3.12) is because these are simple, yet flexible, expressions with an obvious physical interpretation. In particular, the expected repulsion is obtained if $\gamma > 0$ and $\alpha, \beta > 1$. If $\alpha = \beta = \gamma = 1$ there is no interaction. The assumption that ξ_i is Beta-distributed could be replaced by the more general parametric models on the unit inter-

val proposed by Barndorff-Nielsen and Jørgensen (1990). That generalization would not change anything essential in the rest of the paper. Since we require that $b(x, \xi)$ depends only on ξ and its neighbouring dunes in x , (3.8)-(3.12) give

$$\beta(x) = k \sum_{j=0}^n (x_{j+1} - x_j)^\gamma \quad (3.13)$$

for some positive parameter k , i.e.

$$b(x_i, \xi, x_{i+1}) = \frac{k}{B(\alpha, \beta)} (x_{i+1} - x_i)^{\gamma-1} \xi_i^{\alpha-1} (1-\xi_i)^{\beta-1} . \quad (3.14)$$

Secondly, we choose

$$d(x_i, \xi, x_{i+1}) = c(x_{i+1} - x_i)^\varphi (\xi - x_i)^\epsilon (x_{i+1} - \xi)^\delta \quad (3.15)$$

with $c \geq 0$. The following conditions imply repulsion:

$$k, c, \gamma > 0 ; \quad \alpha, \beta > 1 ; \quad \epsilon, \delta < 0 ; \quad \varphi + \epsilon + \delta \leq 0 . \quad (3.16)$$

The latter bound is obtained by rewriting (3.15) as

$$d(x_i, \xi, x_{i+1}) = c(x_{i+1} - x_i)^{\varphi + \epsilon + \delta} \xi_i^\epsilon (1 - \xi_i)^\delta .$$

In Appendix 1 weak sufficient conditions are discussed ensuring the existence and convergence of the process defined by (3.14)-(3.15). For the unique existence we only need that $\gamma \geq 0$. It is intuitively clear that the process explodes with a positive

probability if $\gamma < 0$, because then dunes tend to be born between neighbouring dunes which are close so that there is a positive feed-back. In fact, the process exists uniquely for $\gamma \geq 0$ no matter how the density $h(\cdot|\cdot)$ and the function $d(\cdot,\cdot)$ are specified, since the proof of the unique existence is only based on (3.13). Furthermore, it is proved that the process converges as $t \rightarrow \infty$ to a limit distribution which is the unique equilibrium distribution, if $\epsilon, \delta, \varphi + \epsilon + \delta \leq 0$ and either $\gamma > 0$ or

$$\gamma = 0 \quad \text{and} \quad \frac{c}{k} |S|^{\varphi + \epsilon + \delta} \left[\frac{\epsilon}{\epsilon + \delta} \right]^{\epsilon} \left[\frac{\delta}{\epsilon + \delta} \right]^{\delta} > 1, \quad (3.17)$$

hold where $|S|$ is the length of the interval S . In (3.17), $(\epsilon/(\epsilon + \delta))^{\epsilon} (\delta/(\epsilon + \delta))^{\delta} = 1$ if either ϵ or δ or both are 0. Thus, (3.17) holds e.g. in the uniform case $\gamma = \varphi = \epsilon = \delta = 0$ if and only if $c > k$ or equivalently $\beta(x) < \delta(x)$ where $\beta(x)$ and $\delta(x)$ are the rates for a birth and a death, respectively, cf. (3.2). Under the above mentioned conditions for convergence, the rate of convergence is in fact geometrically fast, cf. Appendix 1.

Finally, we observe that the balance condition (3.7) holds if and only if

$$\alpha - \epsilon = \beta - \delta = \alpha + \beta + \varphi - \gamma. \quad (3.18)$$

We shall denote the common value of these three quantities by κ . When (3.18) holds (3.5) defines the density

$$f(x) = ab^n \prod_{i=0}^n (x_{i+1} - x_i)^{\kappa-1}, \quad x = (x_1, \dots, x_n), \quad (3.19)$$

where a is a normalizing constant and $b = k/(cB(\alpha, \beta))$. The condition (3.6) is satisfied for $\gamma \geq 0$, cf. (A.2) in Appendix 1. Thus, if the conditions given above for convergence into equilibrium hold, (3.19) is the limit distribution of the process. Notice that under (3.19) and conditional on n , the distribution at one particular time of the relative distances $(x_{i+1} - x_i)/(x_{n+1} - x_0)$, $i = 0, \dots, n$, between neighbouring dunes is simply a Dirichlet distribution with parameters (κ, \dots, κ) (n times). Therefore, (3.19) is a density if and only if $\kappa > 0$.

A model comprising y -junctions can be built as a straightforward generalization of the model above. At a y -junction two dunes merge, so after this event the number of dunes has gone down by one. Thus a y -junction is a transition from Ω_n to Ω_{n-1} (for some n) in the general birth-and-death process setup discussed in Subsection 3.1. A very simple model is obtained if it is assumed that one of the merging dunes ends while the other simply continues. In such a model a y -junction is a special kind of death, and the death rate $d(x, \xi)$ of the original model should simply be decomposed in a sum of two terms corresponding to the two kinds of death. A more realistic model is obtained by letting the two merging dunes die and then start a new dune at a random point between them. Models of this more general type are also covered by Preston's (1977) theory. As long as we retain our original birth rate (3.13), the birth-and-death process will exist and be unique no matter how we specify the rate of dune

merger and the probability distribution of the location of the resulting joint dune. This follows from the discussion above of the unique existence of the process without y-junctions. The convergence towards a limit distribution, however, depends on these specifications.

4. Likelihood inference

In this section we derive the likelihood function and a partial likelihood functions for the nearest-neighbour birth-and-death process model described in Subsection 3.2. The partial likelihood function is also relevant to a semi-parametric model more general than the one defined in the previous section and is thus in this sense model robust. It is proved that the maximum likelihood estimates exist with probability one, and conditions for the existence of the maximum partial likelihood estimates are discussed. Consideration of asymptotic properties of estimators and test statistics is postponed to Appendix 2.

4.1. Likelihood functions

For a given air photo of a linear dune field and for $x(t) = (x_1, \dots, x_n)$, let $x_j < \dots < x_{j+p}$ be the positions of the dunes which can be seen on the air photo at time t and define $y(t) = (x_{j+1}, \dots, x_{j+p-1})$, $z(t) = (x_1, \dots, x_{j-1}, x_{j+p+1}, \dots, x_n)$ and $\partial(t) = (x_j, x_{j+p})$ (notice that $\partial(t)$ may consist of two, one or no points). Thus, at time t , $y(t)$ is the position of the dunes which together with their neighbouring dunes can be observed on the air photo. The positions of the most left and most right neighbouring dunes to these dunes are given by $\partial(t)$. In order to eliminate any edge effect we shall consider the process $\{y(t): t \geq 0\}$ conditional on $\{\partial(t): t \geq 0\}$. This conditional process is, for a nearest-neighbour birth-and-death process, independent of the process $\{z(t): t \geq 0\}$.

We need the following notation. Let $t_1 < \dots < t_{m-1}$ be the transition times for $\{(y(t), \vartheta(t)): t \geq 0\}$, and let t_0 and t_m be the first and last time, respectively, where (y, ϑ) is observed on the air photo. Furthermore, let

$$\mathcal{C} = \{1, \dots, m\} ,$$

$$\mathcal{B} = \{i \in \mathcal{C}: \text{a birth happens for } y(t) \text{ at time } t=t_i\} ,$$

$$\mathcal{D} = \{i \in \mathcal{C}: \text{a death happens for } y(t) \text{ at time } t=t_i\} ,$$

and for $i \in \mathcal{C}$ let

$$\Delta_i = t_i - t_{i-1} ,$$

$$(y_{i1}, \dots, y_{in_i}) = y(t_{i-1}) \text{ and } (y_{i0}, y_{i(n_i+1)}) = \vartheta(t_{i-1})$$

$$\text{where } y_{i0} < y_{i1} < \dots < y_{i(n_i+1)} ,$$

$$r_{ij} = y_{i(j+1)} - y_{ij} \text{ for } j = 0, \dots, n_i ,$$

$$s_{ij} = y_{i(j+1)} - y_{i(j-1)} = r_{i(j-1)} + r_{ij} \text{ for } j = 1, \dots, n_i .$$

For $i \in \mathcal{B}$ we define

$$\xi^{(i)} = \text{position of the dune starting at time } t_i ,$$

$$j_i \text{ such that } y_{ij_i} < \xi^{(i)} < y_{i(j_i+1)} ,$$

$$\xi_i = (\xi^{(i)} - y_{ij_i}) / (y_{i(j_i+1)} - y_{ij_i}) ,$$

and for $i \in \mathcal{D}$ we let

j_i be such that y_{ij_i} is the position of the dune which dies at time t_i .

Finally, let

$$g = g(\{Y(t): t \in [t_0, t_m]\} | \{\partial(t): t \in [t_0, t_m]\}, Y(t_0))$$

denote the conditional density of $\{Y(t): t \in [t_0, t_m]\}$ given $\{\partial(t): t \in [t_0, t_m]\}$ and $Y(t_0)$ with respect to the probability measure of the birth-and-death process with $b(\cdot, \cdot) \equiv d(\cdot, \cdot) \equiv 1$, i.e. the process which adds and delete points uniformly.

Now, for any nearest-neighbour birth-and-death process, it follows straightforwardly from (3.1)-(3.4) that

$$\begin{aligned} g = & \prod_{i \in \mathcal{E}} \exp(-\lambda_i \sum_{j=0}^{n_i} H(Y_{ij}, Y_{i(j+1)}) - \lambda_i \sum_{j=1}^{n_i} d(Y_{i(j-1)}, Y_{ij}, Y_{i(j+1)})) \\ & \times \prod_{i \in \mathcal{E}} b(y_{ij_i}, \xi^{(i)}, y_{i(j_i+1)}) \\ & \times \prod_{i \in \mathcal{D}} d(y_{i(j_i-1)}, y_{ij_i}, y_{i(j_i+1)}) \\ & / \prod_{i \in \mathcal{E}} \exp(-\lambda_i (y_{in_{i+1}} - y_{i0}) - \lambda_i n_i) . \end{aligned} \tag{4.1}$$

Combining this with (3.14)-(3.15) we get the likelihood function L for our model, i.e.

$$L = k^{\#\mathcal{G}} c^{\#\mathcal{D}} \exp(-k \sum_{i \in \mathcal{G}} \Lambda_i \sum_{j=0}^{n_i} r_{ij}^\gamma - c \sum_{i \in \mathcal{G}} \Lambda_i \sum_{j=1}^{n_i} s_{ij}^\varphi r_{i(j-1)}^\epsilon r_{ij}^\delta) \quad (4.2)$$

$$\times \prod_{i \in \mathcal{G}} [r_{ij_i}^\gamma \frac{\xi_i^{\alpha-1} (1-\xi_i)^{\beta-1}}{B(\alpha, \beta)}] \prod_{i \in \mathcal{D}} [s_{ij_i}^\varphi r_{i(j_i-1)}^\epsilon r_{ij_i}^\delta] .$$

This factorizes as

$$L = L_1(k, \gamma) L_2(c, \varphi, \epsilon, \delta) L_3(\gamma) L_4(\alpha, \beta) L_5(\varphi, \epsilon, \delta) \quad (4.3)$$

where

$$L_1 = (k \sum_{i \in \mathcal{G}} \Lambda_i \sum_{j=0}^{n_i} r_{ij}^\gamma)^{\#\mathcal{G}} \exp(-k \sum_{i \in \mathcal{G}} \Lambda_i \sum_{j=0}^{n_i} r_{ij}^\gamma) , \quad (4.4)$$

$$L_2 = (c \sum_{i \in \mathcal{G}} \Lambda_i \sum_{j=1}^{n_i} s_{ij}^\varphi r_{i(j-1)}^\epsilon r_{ij}^\delta)^{\#\mathcal{D}} \\ \times \exp(-c \sum_{i \in \mathcal{G}} \Lambda_i \sum_{j=1}^{n_i} s_{ij}^\varphi r_{i(j-1)}^\epsilon r_{ij}^\delta) , \quad (4.5)$$

$$L_3 = \prod_{i \in \mathcal{G}} (r_{ij_i}^\gamma / \sum_{h \in \mathcal{G}} \Lambda_h \sum_{j=0}^{n_h} r_{hj}^\gamma) , \quad (4.6)$$

$$L_4 = \prod_{i \in \mathcal{G}} \frac{\xi_i^{\alpha-1} (1-\xi_i)^{\beta-1}}{B(\alpha, \beta)} , \quad (4.7)$$

$$L_5 = \prod_{i \in \mathcal{D}} (s_{ij_i}^\varphi r_{i(j_i-1)}^\epsilon r_{ij_i}^\delta / \sum_{h \in \mathcal{E}} \Lambda_h \sum_{j=1}^{n_h} s_{hj}^\varphi r_{h(j-1)}^\epsilon r_{hj}^\delta) . \quad (4.8)$$

The profile likelihood function \tilde{L} for the parameters α , β , γ , φ , ϵ and δ is shown in Subsection 4.2 to be

$$\tilde{L} = L_3(\gamma) L_4(\alpha, \beta) L_5(\varphi, \epsilon, \delta) , \quad (4.9)$$

so the maximum likelihood estimates for γ , (α, β) and $(\varphi, \epsilon, \delta)$ can be found from L_3 , L_4 and L_5 , respectively. We shall now introduce a partial likelihood function in the sense of Cox (1975) which, as argued below, turns out to be of a form similar to \tilde{L} in (4.9), namely

$$L_p = L_{p3}(\gamma) L_{p4}(\alpha, \beta) L_{p5}(\varphi, \epsilon, \delta) , \quad (4.10)$$

Here L_{p4} equals L_4 whereas L_{p3} and L_{p5} can be regarded as alternatives to L_3 and L_5 for estimating γ and $(\varphi, \epsilon, \delta)$, respectively. Note that (4.9) and (4.10) still hold if L_4 is replaced by the likelihood function based on another choice of parametric model than the family of Beta-distributions given by (4.7).

The partial likelihood function is obtained by arguing that the waiting times $\mathcal{T} = \{\Lambda_i : i \in \mathcal{E}\}$ and the observations whether each particular transition is a birth or a death do not contain much information about the parameters γ , φ , ϵ and δ , and

obviously no information on α and β . The distribution of this part of the observations depends on the parameters γ , φ , ϵ and δ in quite an intricate way and is mainly determined by k and c . In the general set-up we obtain the partial likelihood function by multiplying first over all births the conditional density of the position of the new dune given the past, i.e. given the configuration immediately prior to the birth, and secondly over all deaths the conditional probability of which dune is dying given the past. Hence we find the following expression for the partial likelihood function:

$$L_p = \prod_{i \in \mathcal{B}} \frac{\prod_{j=0}^{n_i} H(y_{ij_i}, y_{i(j_i+1)})}{\prod_{j=0}^{n_i} H(y_{ij}, y_{i(j+1)})} \prod_{i \in \mathcal{B}} h(x_i | y_{ij_i}, y_{i(j_i+1)}) \\ \times \prod_{i \in \mathcal{D}} \frac{\prod_{j=0}^{n_i} d(y_{i(j_i-1)}, y_{ij_i}, y_{i(j_i+1)})}{\prod_{j=0}^{n_i} d(y_{i(j-1)}, y_{ij}, y_{i(j+1)})}.$$

With our particular specifications (3.14) and (3.15), we find that L_p is given by (4.10) where

$$L_{p3} = \prod_{i \in \mathcal{B}} (r_{ij_i}^\gamma / \prod_{j=0}^{n_i} r_{ij}^\gamma), \quad (4.11)$$

$$L_{p5} = \prod_{i \in \mathcal{D}} (s_{ij_i}^\varphi r_{i(j_i-1)}^\epsilon r_{ij_i}^\delta / \prod_{j=1}^{n_i} s_{ij}^\varphi r_{i(j-1)}^\epsilon r_{ij}^\delta). \quad (4.12)$$

An appealing quality of the partial likelihood function (4.10) is that the same expression would be obtained in the much

larger class of semi-parametric models obtained by allowing k and c to be functions depending on the time and on the entire past of the process. Thus also non-Markovian birth-and-death processes are included. The only restriction on k and c is that the process should not explode. For instance, it suffices to require that k is bounded. Dependence on time would, in the linear dune field context considered particularly in this paper, correspond to a spatial inhomogeneity in the wind direction.

4.2. Estimation

We recall that the nearest-neighbour birth-and-death model given by (3.14)-(3.15) exists if and only if $\gamma \geq 0$, so the variation of the parameters in the full model is given by

$$H_0: k, c > 0, \quad \gamma \geq 0, \quad \alpha, \beta > 0, \quad \varphi, \delta, \epsilon \in \mathbb{R}.$$

In this subsection we shall discuss maximum likelihood estimation under H_0 and under the following simplifications,

$$H_1: \alpha = \beta,$$

$$H_2: \epsilon = \delta,$$

$$H_3: \varphi = -\epsilon - \delta,$$

$$H_4: \alpha - \epsilon = \beta - \delta = \alpha + \beta + \varphi - \gamma = \kappa > 0.$$

The hypotheses H_1 and H_2 specify that the interaction is symmetric between a dune and its nearest left and right neighbouring dunes, cf. (3.12) and (3.15). The hypothesis H_3 states that the tendency of a dune to die depends only on the position of this dune relatively to its neighboring dunes and not separately on the distance between the two neighbouring dunes, cf. (3.15). The hypothesis H_4 is the balance condition (3.18). Note that under H_3 the balance condition H_4 simplifies to $\alpha - \epsilon = \beta - \delta = \gamma = \kappa$.

For fixed $\alpha, \beta, \gamma, \varphi, \epsilon$ and δ the likelihood function L attains, under any of the hypotheses H_0-H_4 , its maximal value at (k, c) given by

$$k(\gamma) = \# \mathcal{B} / \sum_{i \in \mathcal{E}} \Lambda_i \sum_{j=0}^{n_i} r_{ij}^{\gamma}$$

$$c(\varphi, \epsilon, \delta) = \# \mathcal{D} / \sum_{i \in \mathcal{E}} \Lambda_i \sum_{j=0}^{n_i} s_{ij}^{\varphi} r_{i(j-1)}^{\epsilon} r_{ij}^{\delta}$$

cf. (4.3)-(4.5). Thus, given estimates $\hat{\gamma}, \hat{\varphi}, \hat{\epsilon}, \hat{\delta}$ under any of the hypotheses we estimate k and c by

$$\hat{k} = k(\hat{\gamma}), \quad \hat{c} = c(\hat{\varphi}, \hat{\epsilon}, \hat{\delta}). \quad (4.13)$$

Notice that under any of the hypotheses H_0-H_3 (but not H_4) we have that

$$L(\gamma, \alpha, \beta, \varphi, \epsilon, \delta, k(\gamma), c(\varphi, \epsilon, \delta))$$

$$\propto L_3(\gamma)L_4(\alpha,\beta)L_5(\varphi,\epsilon,\delta) ,$$

cf. (4.3)-(4.8). In particular, this proves (4.9). The maximum likelihood estimates of the parameters γ , φ , ϵ and δ and the likelihood ratio statistics for H_2, H_3 and other hypotheses involving only these parameters do not depend on our particular choice of L_4 .

Now, let us discuss the existence of the maximum likelihood estimates and the partial likelihood estimates. Since L_4 is simply the likelihood function for the Beta distributed sample $(\xi_i: i \in \mathcal{I})$, cf. (4.7), it suffices under any of the hypotheses H_0-H_3 to consider the likelihood functions L_3 and L_5 and the alternative partial likelihood functions L_{p3} and L_{p5} . These functions are all of the form

$$m(\theta_1, \dots, \theta_p) = \prod_{i \in \mathcal{I}} \left[1 + \sum_{j \in \mathcal{A}_i} a_{ij} \prod_{k=1}^p v_{ijk}^{\theta_k} \right]^{-1} \quad (4.14)$$

where \mathcal{I} and the \mathcal{A}_i are finite sets, $p < \infty$, $a_{ij} > 0$, $\theta_k \in \mathbb{R}$ and $v_{ijk} \in \mathbb{R}$ for all i, j, k , compare with (4.6), (4.8), (4.11) and (4.12). For instance, (4.6) is of the form (4.14) with $\mathcal{I} = \mathcal{H}$, $\mathcal{A}_i = \{(h, j): h \in \mathcal{H}, j=1, \dots, n_h\} \setminus \{(i, j_i)\}$, $p = 1$, $a_{i(h, j)} = \Lambda_h / \Lambda_i$ and $v_{i(h, j)k} = r_{hj} / r_{ij_i}$. Likelihood functions of the form (4.14) were studied by Jacobsen (1990). From his results it follows that the function $m: \mathbb{R}^p \rightarrow \mathbb{R}_+$ attains its maximal value at a unique point if and only if there does not exist $(\theta_1, \dots, \theta_p) \neq (0, \dots, 0)$ such that

$$\prod_{k=1}^p v_{ijk}^{\theta_k} \geq 1 \quad \text{for all } j \in \mathcal{A}_i \text{ and } i \in \mathcal{I}, \quad (4.15)$$

and in this case the function $\log(m(\cdot))$ is strictly concave.

Consider first the case $m(\gamma) = L_3(\gamma)$. Here (4.15) is satisfied if and only if $r_{hj}^\gamma \geq r_{ij_i}^\gamma$ for all $(h,j) \in \mathcal{A}_i$ and all $i \in \mathcal{I}$, in particular for all (h,j_h) , $h \in \mathcal{I} \setminus \{i\}$. This is only possible in case r_{ij_i} is the same for all $i \in \mathcal{I}$, which happens with probability 0 provided $\#\mathcal{I} > 1$. Thus, if $\#\mathcal{I} > 1$, $L_3(\cdot)$ has a unique maximum and is strictly log-concave almost surely. In particular the maximum likelihood estimate of γ exists almost surely and is easily determined by the Newton-Raphson algorithm. Note, however, that $\hat{\gamma}$ might be negative which corresponds to an exploding process. It is analogously seen that the maximum likelihood estimates of the other parameters exist almost surely under any of the hypotheses H_0 - H_3 if $\#\mathcal{I} > 1$ and $\#\mathcal{D} > 1$. The estimates can be found easily by maximizing (4.6)-(4.8), which are almost surely log-concave, and then substituting in (4.13).

The maximum partial likelihood estimates based on (4.11)-(4.12) exist with a probability less than one under any of the hypotheses H_0 - H_3 . For instance, it is seen from (4.15) that the maximum partial likelihood estimate of γ does not exist if and only if either $r_{ij_i} \leq r_{ij}$ for all $i \in \mathcal{I}$ and $j = 0, \dots, n_i$ or $r_{ij_i} \geq r_{ij}$ for all $i \in \mathcal{I}$ and $j = 0, \dots, n_i$. That is, the only situations in which the maximum partial likelihood estimate of γ

does not exist is either when all births take place between the two dunes with the largest spacing or when all births take place in the smallest dune interval available. The probability of this event tends to zero as $\#B$ tends to infinity. It follows analogously that the maximum partial likelihood estimates of the parameters φ , ϵ and δ exist on an event which is, in general, more complicated, but easily described in terms of (4.15). Under H_2 and H_3 it is easily seen that the maximum partial likelihood estimate does not exist if and only if either all deaths happen to the dune for which $r_{i(j_i-1)} r_{ij_i} s_{ij_i}^{-2}$ is largest, or all deaths happen to the dune with the minimum value of $r_{i(j_i-1)} r_{ij_i} s_{ij_i}^{-2}$. The probability of this event tends to zero as $\#D$ tends to infinity.

Under the hypothesis H_4 , combined with one or more of the hypotheses H_0 - H_3 , the profile likelihood function \tilde{L} in (4.9) can, for fixed α and β , be shown to have the form (4.14). Using (4.15) it turns out that it attains its unique maximum with probability one if $\#B > 1$ and $\#D > 1$. Therefore, in order to find the maximum likelihood estimates under H_4 , one can simply investigate

$$\max_{\gamma \geq 0, \kappa > 0} L_3(\gamma) L_4(\alpha, \beta) L_5(\gamma + \kappa - \alpha - \beta, \alpha - \kappa, \beta - \kappa)$$

as a function of (α, β) . The maximum can, for each value of (α, β) , be determined by the Newton-Raphson algorithm.

It seems likely that the asymptotic normality of the maximum likelihood estimators and the partial maximum likelihood estima-

tors can be proved using the fact that the score functions and partial score function under the various models are martingales. This and other asymptotic problems are discussed, but not proved, in Appendix 2.

5. Analysis of air photo data

In this section we analyse statistically the air photo data using the nearest-neighbour birth-and-death process model discussed in the previous sections. It should be noted that proofs are not given in this paper of asymptotic results justifying our use of confidence intervals based on the observed information and of χ^2 -approximations to distributions of test statistics. Asymptotic results are discussed in Appendix 2.

Table 5.1 gives the maximum likelihood estimates of the model parameters for the data in image 14a and image 15 under the hypotheses H_0 , H_1+H_2 and $H_1+H_2+H_3$. Also confidence intervals are given for the most important parameters. These intervals are based on the observed information evaluated at the maximum likelihood estimates. The interval for γ is derived from the profile information, but this is well-known to give the correct result, see Richards (1961) and Patefield (1977).

The estimates in Table 5.1 satisfy condition (3.16) implying that the interaction between neighbouring dunes is a repulsion as expected. Also the condition which implies geometrically fast convergence into equilibrium, cf. Section 3.2, is satisfied. A glance at Table 5.1 is enough to expect the hypotheses H_1 and H_2 of symmetry to be acceptable, and indeed the loglikelihood ratio test statistic for H_1 under H_0 is $-2 \log Q = 0.05$ for image 14a and $-2 \log Q = 0.01$ for image 15. The corresponding observed levels of significance, using the $\chi^2(1)$ -distribution, are 82% and 92%. When testing H_2 under H_0 we find $-2 \log Q = 0.09$ for image 14a and $-2 \log Q = 0.30$ for image 15 corresponding to the levels of significance 76% and 59%, respectively.

	α	β	γ	δ	ϵ	φ	k	c
Image 14a								
H_0	2.87	2.80	3.13 ± 0.64	-1.52 ± 1.07	-1.63 ± 1.23	2.29 ± 2.30	$8.93 \cdot 10^{-8}$	$5.48 \cdot 10^{-3}$
$H_1 + H_2$	2.83		3.13 ± 0.64	-1.54 ± 1.05		2.19 ± 2.18	$8.93 \cdot 10^{-8}$	$6.13 \cdot 10^{-3}$
$H_1 + H_2 + H_3$	2.83		3.13 ± 0.64	-1.37 ± 1.05			$8.93 \cdot 10^{-8}$	$3.19 \cdot 10^{-4}$
Image 15								
H_0	2.32	2.28	2.16 ± 0.58	-1.92 ± 0.85	-2.08 ± 0.91	3.26 ± 1.68	$1.91 \cdot 10^{-7}$	$2.19 \cdot 10^{-3}$
$H_1 + H_2$	2.30		2.16 ± 0.58	-1.96 ± 0.81		3.19 ± 1.65	$1.91 \cdot 10^{-7}$	$2.24 \cdot 10^{-3}$
$H_1 + H_2 + H_3$	2.30		2.16 ± 0.58	-1.74 ± 0.86			$1.91 \cdot 10^{-7}$	$1.13 \cdot 10^{-4}$

Table 5.1. Maximum likelihood estimates of the model parameters for the data in image 14a and image 15 under the hypotheses H_0 , $H_1 + H_2$ and $H_1 + H_2 + H_3$. The confidence intervals are based on the observed information.

	γ	δ	ϵ	φ	k	c
Image 14a						
H_0	3.89 ± 0.97	-2.30 ± 1.55	-2.39 ± 1.55	3.89 ± 3.09	$5.22 \cdot 10^{-9}$	$1.28 \cdot 10^{-3}$
H_2	3.89 ± 0.97	-2.34 ± 1.51		3.88 ± 3.10	$5.22 \cdot 10^{-9}$	$1.26 \cdot 10^{-3}$
H_2+H_3	3.89 ± 0.97	-2.23 ± 1.53			$5.22 \cdot 10^{-9}$	$7.82 \cdot 10^{-5}$
Image 15						
H_0	2.32 ± 0.68	-1.81 ± 1.45	-1.94 ± 1.49	2.93 ± 2.73	$9.24 \cdot 10^{-8}$	$3.83 \cdot 10^{-3}$
H_2	2.32 ± 0.68	-1.85 ± 1.43		2.88 ± 2.73	$9.24 \cdot 10^{-8}$	$4.01 \cdot 10^{-3}$
H_2+H_3	2.32 ± 0.68	-1.50 ± 1.29			$9.24 \cdot 10^{-8}$	$1.67 \cdot 10^{-4}$

Table 5.2. Maximum partial likelihood estimates under the hypotheses H_0 , H_2 and H_2+H_3 of γ , δ , ϵ and φ and the corresponding estimates of k and c obtained by substitution in (4.13). The estimates are based on the data in image 14a and image 15. The confidence intervals are based on the observed partial likelihood information.

It is not obvious from Table 5.1 whether H_3 is acceptable or not, and the log-likelihood ratio tests do not give a clear answer to the question. The test statistics for testing H_3 under H_2 are, for the two images, $-2 \log Q = 3.60$ and $-2 \log Q = 3.65$, respectively. Both these values correspond to an observed significance level of about 6%, so we do not have much faith in H_3 .

In Table 5.2 the partial likelihood estimates are given together with confidence intervals based on the observed partial likelihood information. These estimates are rather different from the maximum likelihood estimates, but they also satisfy the conditions for repulsion between neighbouring dunes and for geometrically fast convergence into equilibrium. It is interesting that the estimates of the sum $\delta + \epsilon + \varphi$ vary only by 0.1 at most between the two tables. The confidence intervals in Table 5.2 are consistently larger than those in Table 5.1 indicating a loss of information in using the partial likelihood function. We shall discuss the partial likelihood estimates further in Section 6.

Under the hypothesis $H_1 + H_2$ the structure of a linear dune field is described by six parameters $k, c, \alpha, \gamma, \delta$ and $\varphi + 2\delta$ which we can use for comparing the two images 14a and 15. The maximum likelihood estimates of the last parameter are -0.89 (image 14a) and -0.73 (image 15), so in this respect the two parts of the dune field do not differ. The variation of $\hat{\delta}$ is obviously not significant. On the other hand, the estimates of γ vary considerably from one image to the other.

Let us finally consider the balance condition H_4 . Under this condition the spatial birth-and-death process is time reversible, i.e. the dune field looks the same whether you walk through it in the wind direction or against the wind. Rejection of this hypothesis would substantiate the theory that linear dune fields develop in the wind direction. Under H_1 and H_2 the hypothesis H_4 states that $\alpha + \varphi + \epsilon - \gamma = 0$. From Table 5.1 we see that the maximum likelihood estimates of this sum are 0.35 and 1.37 for image 14a and image 15, respectively. The log-likelihood ratio statistics for testing H_4 under $H_1 + H_2$ are, for each of the two images, $-2 \log Q = 0.15$ and $-2 \log Q = 3.41$. If we evaluate these statistics in the $\chi^2(1)$ -distribution, we find that the observed levels of significance are 70% and 7% for image 14a and image 15, respectively. We can not believe strongly in the hypothesis of the reversibility in the part of the dune field on image 15.

6. Model control

In this section we propose various plots to be used for checking that the data fit our model reasonably. The developed graphical techniques are tried out on our dune field data, image 14a and image 15.

The exponential distribution of the waiting times between events can be checked by means of a P-P plot of the observed waiting times conditionally on the boundary events $\{\partial(t): t \geq 0\}$. These waiting times are not exponentially distributed. For each $i \in \mathbb{N}$ define the number $k(i) < i$ by $k(i) \in \mathbb{N}$ and $k(i) < j < i \Rightarrow j \notin \mathbb{N}$. Thus the time between the birth or death at time t_i and the last birth or death before t_i that was not a boundary event is $t_i - t_{k(i)}$. The integrated hazard of the distribution of this waiting time, evaluated at $t_i - t_{k(i)}$ is

$$\Lambda_i = \sum_{j=k(i)+1}^i \Lambda_j \left\{ \sum_{m=0}^{n_j} H(y_{jm}, y_{j(m+1)}) + \sum_{m=1}^{n_j} d(y_{j(m-1)}, y_{jm}, y_{j(m+1)}) \right\}, \quad (6.1)$$

conditionally on the state at time $t_{k(i)}$. Here H and d are given by (3.11), (3.13) and (3.15). Hence $\exp(-\Lambda_i)$ is, under the same condition, uniformly distributed in the interval $[0,1]$. Since this distribution does not depend on the condition, it follows that unconditionally the random variables $\exp(-\Lambda_i)$, $i \in \mathbb{N}$, are uniformly distributed in $[0,1]$. It can also be seen that these random variables are independent. In Figure 6.1 P-P plots based on the observed values of $\exp(-\Lambda_i)$ using the maximum likelihood estimates of the parameters under the full model

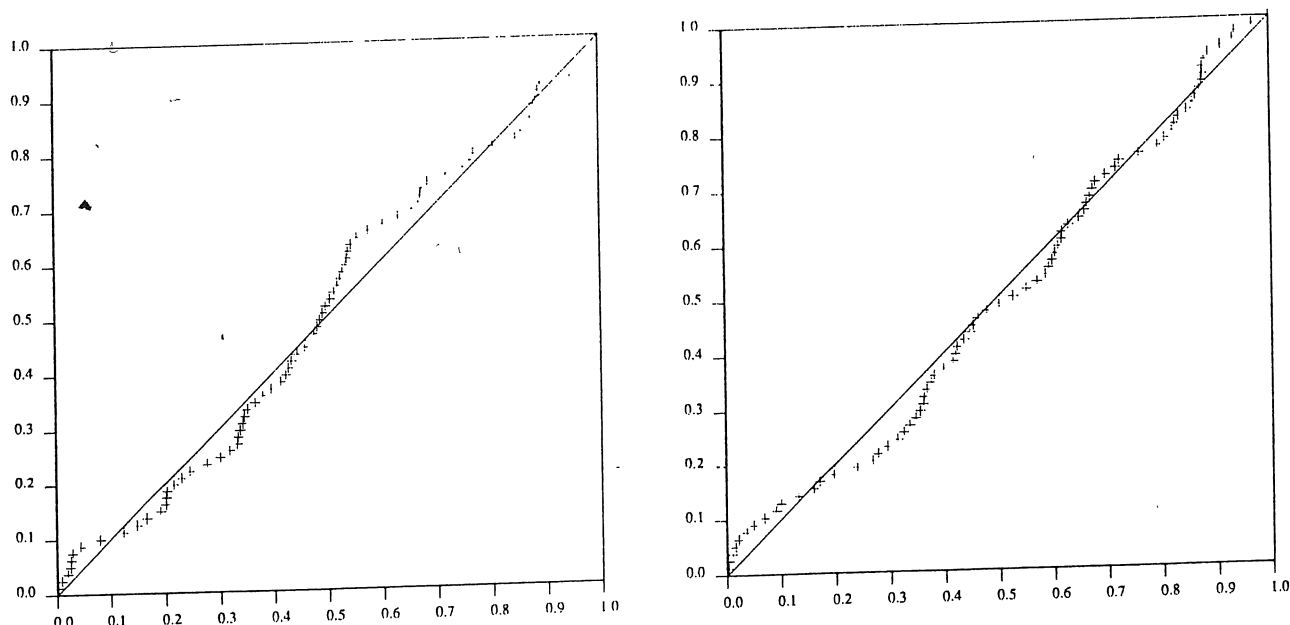


Figure 6.1. Image 14a (left) and Image 15 (right). Graphical check of the exponential distribution of the waiting times by means of a P-P plot of the observed values of $\exp(-\lambda_i)$.

are given for the two images. There are no systematic departures from the identity line.

The probability that event number i is a birth given that $i \in \mathcal{B} \cup \mathcal{D}$ and conditionally on the state at time t_{i-1} is

$$p_i = \frac{\sum_{j=0}^{n_i} H(y_{ij}, y_{i(j+1)})}{\sum_{j=0}^{n_i} H(y_{ij}, y_{i(j+1)}) + \sum_{j=1}^{n_i} d(y_{i(j-1)}, y_{ij}, y_{i(j+1)})} \quad (6.2)$$

Consider the normalized birth indicators

$$z_i = \frac{1_{\{i \in \mathcal{B}\}} - p_i}{\sqrt{p_i(1-p_i)}} \quad i \in \mathcal{B} \cup \mathcal{D} . \quad (6.3)$$

A martingale central limit theorem indicates, see Appendix 2, that if our model is correct, then

$$u = (\#\mathcal{B} + \#\mathcal{D})^{-\frac{1}{2}} \sum_{i \in \mathcal{B} \cup \mathcal{D}} z_i \quad (6.4)$$

is asymptotically standard normally distributed as $\#\mathcal{B} + \#\mathcal{D}$ tends to infinity. Thus u can be used as a goodness-of-fit test statistic. For image 14a we find under H_0 that $u = 0.49$, while $u = -0.07$ for image 15.

Next we shall investigate whether (3.11) is a reasonable model for the probability that a new dune starts in the i 'th interdune interval given that a birth does take place. The distribution function of the length r_{ij_i} (see Section 4) of the interval in which the birth labelled $i \in \mathcal{B}$ takes place is

$$F_i(x) = \frac{n_i}{\sum_{j=0}^{\infty} n_j} r_{ij}^\gamma 1_{\{r_{ij} \leq x\}} \left[\frac{n_i}{\sum_{m=0}^{\infty} n_m} r_{im}^\gamma \right]^{-1} \quad (6.5)$$

conditionally on the state at time t_{i-1} . Appealing to the law of large numbers for martingales, see Appendix 2, we expect that $H(x) \doteq F(x)$ as the number of births tends to infinity, where

$$H(x) = (\#\mathcal{B})^{-1} \sum_{i \in \mathcal{B}} 1_{\{r_{ij_i} \leq x\}} \quad (6.6)$$

and

$$F(x) = (\#\mathcal{J})^{-1} \sum_{i \in \mathcal{J}} F_i(x) . \quad (6.7)$$

We can therefore make a generalized P-P plot by plotting the points $(H(r_{ij_i}), F(r_{ij_i}))$, $i \in \mathcal{J}$. This is done in Figure 6.2 using the maximum likelihood estimates under the full model.

A similar generalized P-P plot can be made for the deaths. By arguments analogous to those given for (6.6) and (6.7) we expect that, for large values of $\#\mathcal{D}$, $G(x) \doteq D(x)$. Here

$$G(x) = (\#\mathcal{D})^{-1} \sum_{i \in \mathcal{D}} 1_{\{s_{ij_i} \leq x\}} \quad (6.8)$$

and

$$D(x) = (\#\mathcal{D})^{-1} \sum_{i \in \mathcal{D}} D_i(x) , \quad (6.9)$$

where

$$D_i(x) = \sum_{j=1}^{n_i} s_{ij}^{\varphi} r_{i(j-1)}^{\epsilon} r_{ij}^{\delta} 1_{\{s_{ij} \leq x\}} \left[\sum_{m=0}^{n_i} s_{im}^{\varphi} r_{i(m-1)}^{\epsilon} r_{im}^{\delta} \right]^{-1} \quad (6.10)$$

is the distribution function of s_{ij_i} given the state at time t_{i-1} . Another possibility is to base the generalized P-P-plot on r_{ij_i}/s_{ij_i} , $i \in \mathcal{D}$, instead of s_{ij_i} , $i \in \mathcal{D}$. In Figure 6.3 the points plotted using the maximum likelihood estimates under the full model.

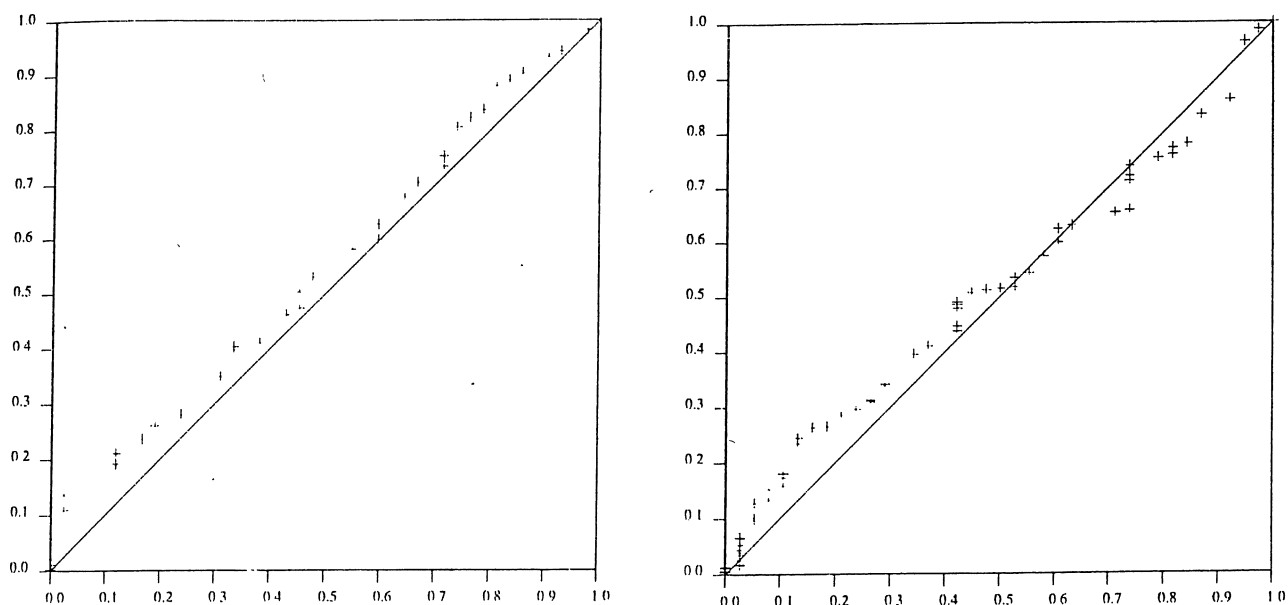


Figure 6.2. Image 14a (left) and Image 15 (right). Graphical check of (3.11) by means of a generalized P-P plot of $(H(r_{ij_i}), F(r_{ij_i}))$, $i \in \mathcal{D}$, given by (6.6) and (6.7). The maximum likelihood estimates of the parameters are used.

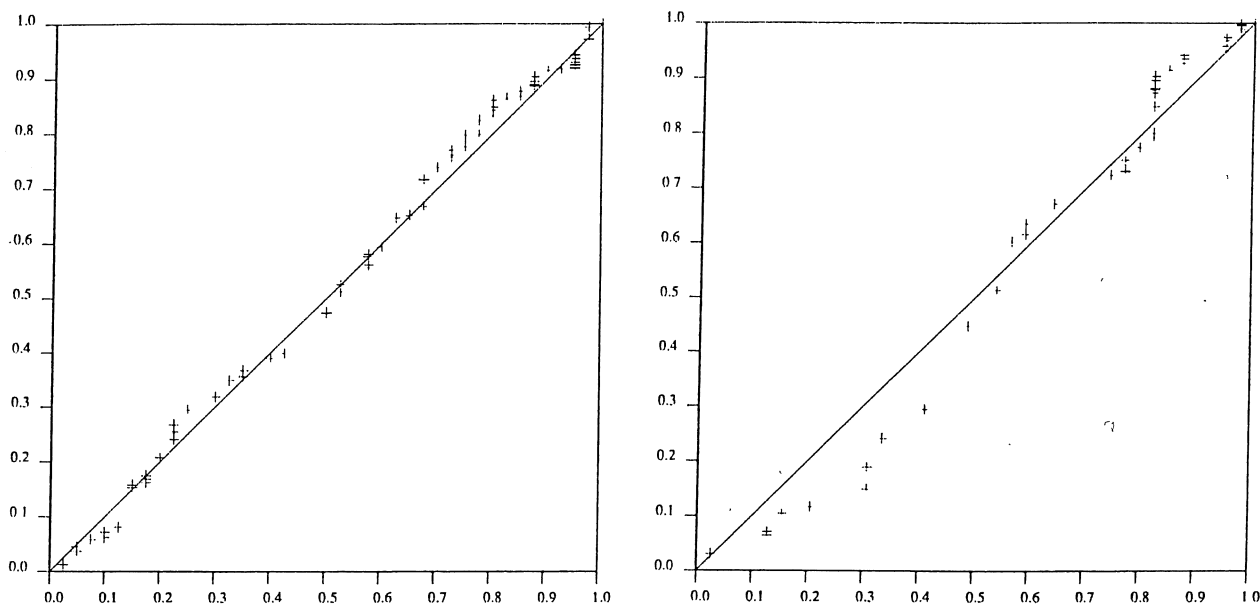


Figure 6.3. Image 14a (left) and Image 15 (right). Graphical check of (3.4) with d defined by (3.15) by means of a generalized P-P plot of $(G(S_{ij_i}), D(S_{ij_i}))$, $i \in \mathcal{D}$, given by (6.8) and (6.9). The maximum likelihood estimates of the parameters are used.

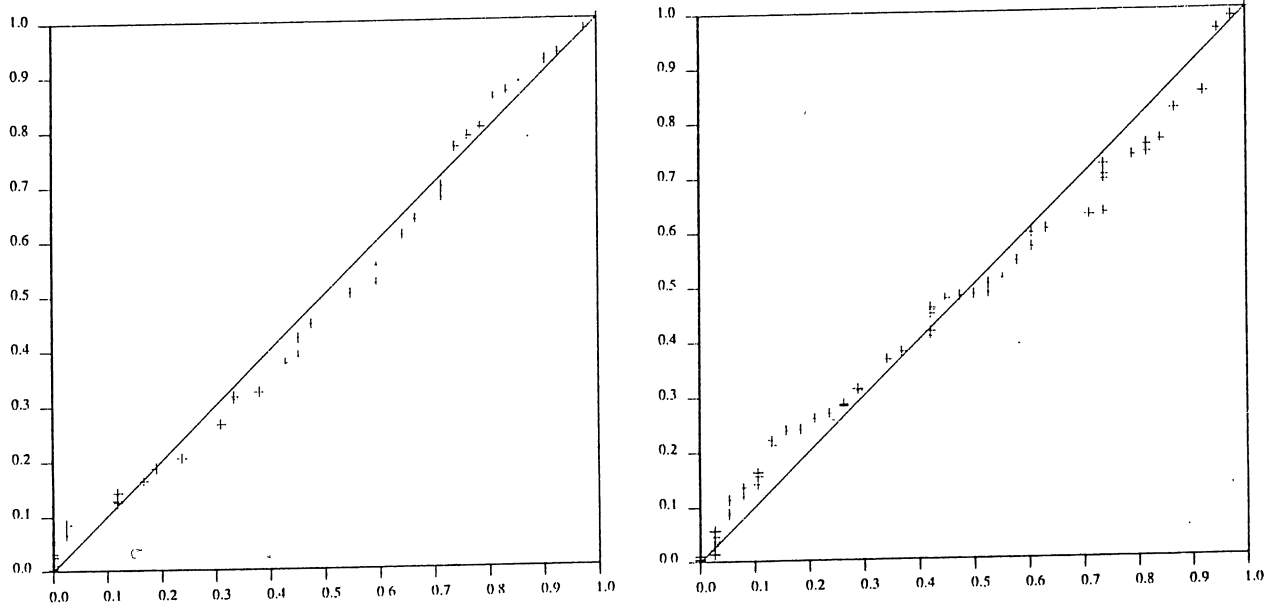


Figure 6.4. Same as Figure 6.2, but the maximum partial likelihood estimates of the parameters are used.

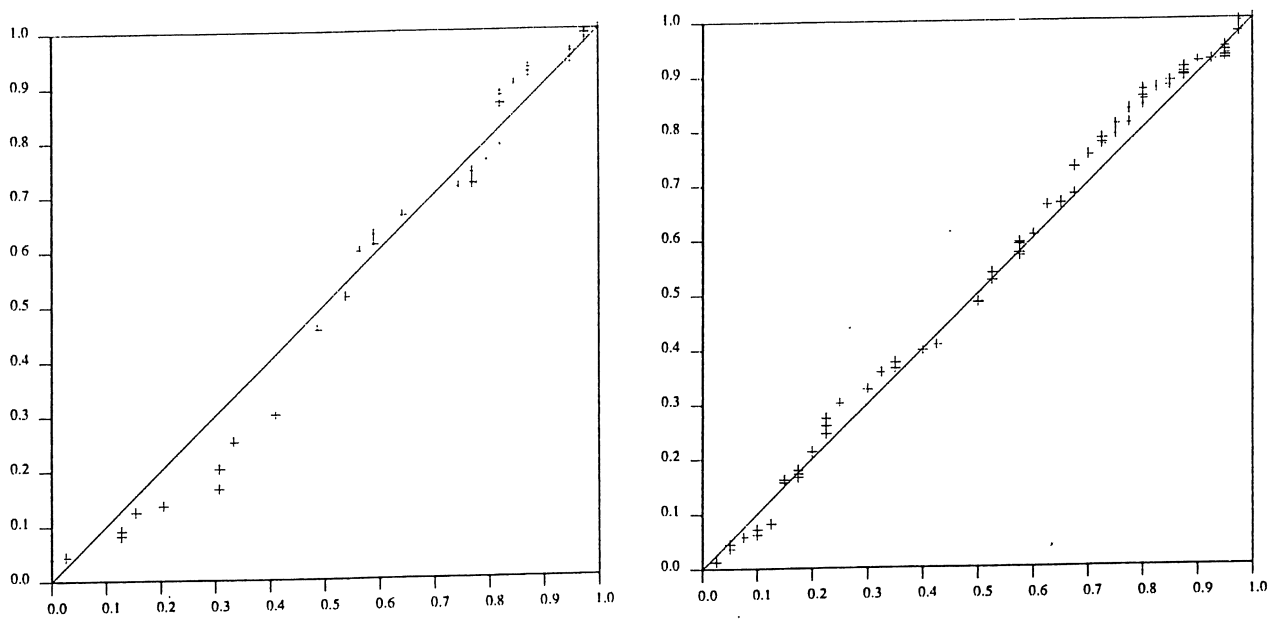


Figure 6.5. Same as Figure 6.3, but the maximum partial likelihood estimates of the parameters are used.

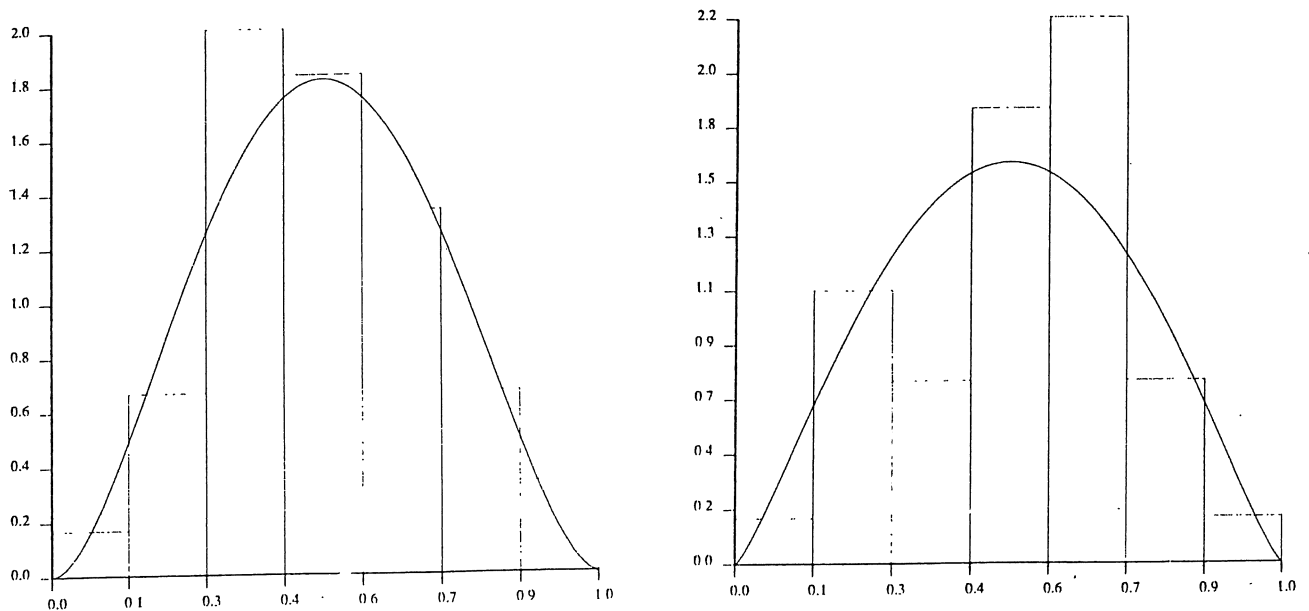


Figure 6.6 . Image 14a (left) and Image 15 (right). Histogram of relative positions of new-born dunes and the estimated symmetrical Beta-density.

The fit in the Figures 6.2 and 6.3 is satisfactory. However, a somewhat better fit is obtained by using the maximum partial likelihood estimates as appears from the Figures 6.4 and 6.5. This is to be expected as the partial likelihood function is based on exactly the aspects of the model that are checked by means of the generalized P-P plots in Figures 6.2-6.5.

Finally, we check the assumption that the relative position of a new-born dune is Beta-distributed by a traditional histogram. In Figure 6.6 histograms of the relative positions ξ_i of new dunes, as defined after (3.12), are plotted together with the

estimated beta-densities under the hypothesis of symmetry $\alpha = \beta$.
The fit is satisfactory - most so for image 14a.

7. Extensions

In this section we briefly discuss extensions of the model in Section 3.2 to birth-and-death processes in higher dimensions. We consider processes where the points are elements of a convex set $S \subseteq \mathbb{R}^k$, i.e. where the state of the process is in S^n , for some $n = 0, 1, 2, \dots$ ($S^0 = \emptyset$). We use a notation which in an obvious way generalizes that of Section 3.

One generalization that is computationally manageable is the following. Assume that any state $x = (x_1, \dots, x_n) \in S^n$ of the process is with probability one in quadratic general position, that is no $s+2$ points of x lie on the same s -dimensional affine subspace, $1 \leq s \leq k-1$, and no $k+2$ points of x lie on the boundary of the same ball in \mathbb{R}^k . This is for example the case if the process is absolutely continuous with respect to the usual Poisson process on S . Further, each state x in general quadratic position defines a Delaunay tessellation with cells D_i , $i = 1, \dots, m(x)$, say. Such a Delaunay cell is the convex hull of $k+1$ points in x which satisfy that the closed ball which contains these $k+1$ points in its boundary do not contain any further points from x . Furthermore, $m(x)$ is the number of all such possible combinations of $k+1$ points from x .

Now, set the birth intensity equal to

$$\beta(x) = k \sum_{i=1}^{m(x)} |D_i|^\gamma, \quad \gamma \in \mathbb{R}, \quad k \geq 0, \quad (7.1)$$

where $|D_i|$ denotes the volume of D_i , and let the probability

that the birth occurs in the cell D_i be proportional to $|D_i|^\gamma$. We also need a probability density on D_i specifying how the exact location of the new point is chosen. An obvious generalization of the Beta-distribution of our one dimensional model would be the following. A disjoint partitioning of D_i in simplexes is obtained by connecting a point ξ in D_i to the vertices of D_i . A probability distribution for ξ is specified by assuming that the volumes of these simplexes divided by $|D_i|$ follows a Dirichlet distribution. Instead of the class of Dirichlet distributions the more general class of parametric models on the simplex proposed by Barndorff-Nielsen and Jørgensen (1990) could be used.

In order to specify the death intensity, we let D_{ij} , $j = 1, \dots, m_i$, denote the Delaunay cells that have point number i as a vertice and D_i the union of these cells. We define the death intensity by

$$\delta(x) = c \sum_{i=1}^n |D_i|^\varphi \prod_{j=1}^{m_i} |D_{ij}|^\epsilon, \quad (7.2)$$

and require that the probability that point number i dies be proportional to $|D_i|^\varphi \prod_{j=1}^{m_i} |D_{ij}|^\epsilon$. Of course, one could, if need be, build asymmetry into the model. Many of the results of the present paper could be generalized to the model thus specified.

In applications we feel that it will often be difficult to interpret the Delaunay cells in dimensions higher than one.

Therefore, models based on Voronoi tessellations, with their obvious physical interpretation, would presumably have wider practical application. Here each point x_i from a given state $x = (x_1, \dots, x_n) \in S^n$ defines a Voronoi cell, which consists of all those points in S which are closer to x_i than to x_j , $j \neq i$. An interesting spatial birth-and-death process Voronoi model appears from (7.1) and (7.2) if we let $D_i = D_i$ denote the Voronoi cell defined by x_i and D_{ij} , $j = 1, \dots, m_i$, the neighbouring cells to D_i . Although this and similar Voronoi models do not include the model in Section 3.2 as a special case, many of the suggested methods in this paper might obviously be used for these Voronoi models.

Acknowledgements: We are grateful to Nick Lancaster for putting the air photos at our disposal and to him and Haim Tsoar for directing our interest towards the dynamics of linear dune fields.

Appendix 1. Existence and convergence of the model given by (3.14) and (3.15)

The spatial birth-and-death process given by (3.14) and (3.15) exists uniquely if

$$\beta_n > 0 \text{ for all } n \geq 0 \text{ and } \sum_{n=0}^{\infty} 1/\beta_n = \infty \quad (\text{A1.1})$$

where

$$\beta_n = \sup_{x \in \Omega_n} \beta(x) ,$$

cf. Preston (1977). By (3.13),

$$\beta_n = k \sup_{x \in \Omega_n} \sum_{i=0}^n (x_{i+1} - x_i)^\gamma .$$

From this we get

$$\beta_n = \begin{cases} k|S|^\gamma (n+1)^{1-\gamma} & \text{if } 0 \leq \gamma \leq 1 \\ k|S|^\gamma & \text{if } \gamma > 1 \end{cases} \quad (\text{A1.2})$$

so (A1.1) is seen to hold for $\gamma \geq 0$. Here $|S|$ denotes the length of the interval S .

The spatial birth-and-death process converges in distribution as $t \rightarrow \infty$ and the limit of the process is the unique equi-

librium distribution provided the following conditions hold (Preston, 1977):

$$\delta_n > 0 \text{ for all } n \geq 1 \text{ and } \sum_{n=1}^{\infty} \frac{\beta_0 \cdots \beta_{n-1}}{\delta_1 \cdots \delta_n} < \infty, \quad (\text{A1.3})$$

$$\sum_{n=1}^{\infty} \frac{\delta_1 \cdots \delta_n}{\beta_1 \cdots \beta_n} = \infty, \quad (\text{A1.4})$$

where

$$\delta_n = \inf_{x \in \Omega_n} \delta(x).$$

We have,

$$\delta_n = c \inf_{x \in \Omega_n} \sum_{i=1}^n (x_{i-1} - x_i)^\epsilon (x_{i+1} - x_i)^\delta (x_{i+1} - x_{i-1})^\varphi,$$

cf. (3.15). For $\epsilon, \delta, \varphi + \epsilon + \delta \leq 0$ a lower limit of δ_n is obtained by

$$\delta_n \geq c |S|^{\varphi + \epsilon + \delta} \inf_{x \in \Omega_n} \sum_{i=1}^n \left[\frac{x_{i-1} - x_i}{x_{i+1} - x_{i-1}} \right]^\epsilon \left[\frac{x_{i+1} - x_i}{x_{i+1} - x_{i-1}} \right]^\delta \quad (\text{A1.5})$$

$$\geq c |S|^{\varphi + \epsilon + \delta} n \left[\frac{\epsilon}{\epsilon + \delta} \right]^\epsilon \left[\frac{\delta}{\epsilon + \delta} \right]^\delta$$

taking $\left[\frac{\epsilon}{\epsilon + \delta} \right]^\epsilon \left[\frac{\delta}{\epsilon + \delta} \right]^\delta = 1$ if either ϵ or δ or both are 0.

Now, if $\gamma \geq 0$ and $\epsilon, \delta, \varphi + \epsilon + \delta \leq 0$, (A1.2) and (A1.5) give

$$\sum_{n=1}^{\infty} \frac{\beta_0 \cdots \beta_{n-1}}{\delta_1 \cdots \delta_n} \leq \begin{cases} \sum_{n=1}^{\infty} \prod_{j=1}^n \frac{m}{j^{\gamma}} & \text{for } 0 \leq \gamma \leq 1 \\ \sum_{n=1}^{\infty} \prod_{j=1}^n \frac{m}{j} & \text{for } \gamma > 1 \end{cases} \quad (\text{A1.6})$$

and

$$\sum_{n=1}^{\infty} \frac{\delta_1 \cdots \delta_n}{\beta_1 \cdots \beta_n} \geq \begin{cases} \sum_{n=1}^{\infty} m^{-n} \frac{[(n+1)!]^{\gamma}}{n+1} & \text{for } 0 \leq \gamma \leq 1 \\ \sum_{n=1}^{\infty} m^{-n} n! & \text{for } \gamma > 1 \end{cases}$$

where

$$m = \frac{k|S|^{\gamma - \varphi - \epsilon - \delta}}{c \left[\frac{\epsilon}{\epsilon + \delta} \right]^{\epsilon} \left[\frac{\delta}{\epsilon + \delta} \right]^{\delta}} > 0.$$

Thus (A1.3) and (A1.4) follow if $\epsilon, \delta, \varphi + \epsilon + \delta \leq 0$ and either $\gamma > 0$ or $m < 1$ for $\gamma = 0$. In fact under these conditions the convergence is geometrically fast. This follows easily by combining (A1.2), (A1.5) and (A1.6) with Corollary 3.2 in Møller (1989).

Appendix 2. Asymptotic results

In this appendix we discuss asymptotic results concerning the statistical procedures proposed in the paper. We shall not prove the results, but rather expose the structure of the problem. We do this by mainly considering statistical inference for (k, γ) . Under the hypotheses H_0-H_3 it makes sense to consider the parameter vector (k, γ) separately because it is L -independent of the other parameters and thus observed orthogonal to these (see e.g. Barndorff-Nielsen (1978)).

Score functions are, under very mild regularity conditions, martingales, see Barndorff-Nielsen and Sørensen (1989). So also for our models. Suppose the birth-and-death process has been observed in the time interval $[t_0, t]$. Then the corresponding score vectors are martingales as functions of t . To see this define the sets

$$\mathcal{C}_t = \{i \in \mathcal{C} : t_i \leq t\}$$

and

$$\mathcal{B}_t = \mathcal{B} \cap \mathcal{C}_t.$$

The notation is as in Section 4. The score vector for (k, γ) is given by

$$\frac{\partial l}{\partial k} = \dot{l}_k = \frac{\#\mathcal{B}_t}{k} - \sum_{i \in \mathcal{C}_t} \Lambda_i \sum_{j=0}^{n_i} r_{ij}^{\gamma} \quad (\text{A2.1})$$

A2.2

$$\frac{\partial l}{\partial \gamma} = \dot{l}_\gamma = \sum_{i \in \mathcal{E}_t} \log(r_{ij_i}) - k \sum_{i \in \mathcal{E}_t} \Lambda_i \sum_{j=0}^{n_i} r_{ij}^\gamma \log(r_{ij}) , \quad (\text{A2.2})$$

where l denotes the log likelihood function, cf. (4.3), (4.4) and (4.6). Define the counting processes

$$N_t = \#\mathcal{E}_t$$

and

$$x_t^p = \#\{i: i \in \mathcal{E}_t, j_i = p\} .$$

The last process has the predictable intensity

$$\lambda_t^p = k R_p(N_{t-})^\gamma ,$$

where $R_j(i) = r_{(i+1)j}$ if $j \leq n_{i+1}$ and $R_j(i) = 0$ otherwise.

Hence

$$m_t^p = x_t^p - \int_0^t \lambda_s^p ds$$

is a martingale with respect to the filtration generated by the entire history of the birth-and-death process. This is provided we set (k, γ) equal to the true value (k_0, γ_0) . We have used that $0 \leq R_j(i) \leq |S|$ so that λ_t^p is bounded (we consider only the non-explosive case $\gamma_0 \geq 0$). From the considerations above it follows that \dot{l}_k and \dot{l}_γ are martingales when evaluated at (k_0, γ_0) since

$$i_k = k^{-1} \sum_{p=0}^{\infty} m_t^p \quad (\text{A2.3})$$

$$i_\gamma = \sum_{p=0}^{\infty} \int_0^t \log(R_p(N_{s-})) dm_s^p. \quad (\text{A2.4})$$

The sums are finite for all t and we set $0 \log 0 = 0$. Similar considerations can be used to show that the entire score vector is a vector martingale as a function of the observation time t under any of the hypotheses H_0-H_4 .

The logarithm of the partial likelihood function for γ under H_0-H_3 differentiated with respect to γ equals

$$i_p(\gamma) = \sum_{i \in \mathcal{B}_t} \{ \log(r_{ij_i}) - E_i(\log(r_{ij_i}); \gamma) \} \quad (\text{A2.5})$$

where

$$E_i(\log(r_{ij_i}); \gamma) = \frac{\sum_{j=0}^{n_i} r_{ij}^\gamma \log(r_{ij})}{\sum_{j=0}^{n_i} r_{ij}^\gamma} \quad (\text{A2.6})$$

is the expectation of $\log(r_{ij_i})$ conditional on the state at time t_{i-1} for the parameter value γ . The process $i_p(\gamma_0)$, indexed by \mathcal{B} , is a discrete time martingale with respect to the filtration $\mathcal{F}_i = \sigma$ (history of the birth-and-death process in the time interval $[t_0, t_{i-1}]$), $i \in \mathcal{B}$. The partial score derived from (4.12) is a discrete time martingale indexed by the number of deaths in a similar way.

A2.4

Asymptotic results follow from the martingale properties of the score functions by standard methods (see e.g. Barndorff-Nielsen and Sørensen (1989)). In order to prove the asymptotic results it must be verified that for γ in an open interval I containing the true value γ_0

$$t^{-1} \sum_{i \in \mathcal{C}_t} \Lambda_i \sum_{j=1}^{n_i} r_{ij}^{\gamma} \rightarrow g_1(\gamma) \quad (\text{A2.7})$$

$$t^{-1} \sum_{i \in \mathcal{C}_t} \Lambda_i \sum_{j=1}^{n_i} r_{ij}^{\gamma} \log(r_{ij}) \rightarrow g_2(\gamma) \quad (\text{A2.8})$$

$$t^{-1} \sum_{i \in \mathcal{C}_t} \Lambda_i \sum_{j=1}^{n_i} r_{ij}^{\gamma} [\log(r_{ij})]^2 \rightarrow g_3(\gamma) > 0 \quad (\text{A2.9})$$

in quadratic mean as $t \rightarrow \infty$ and that the un-normalized sums tend to infinity almost surely for $\gamma = \gamma_0$. Moreover, we need that

$$G(k, \gamma) = \begin{Bmatrix} k^{-1}g_1(\gamma) & g_2(\gamma) \\ g_2(\gamma) & kg_3(\gamma) \end{Bmatrix}$$

is positive definite at $(k, \gamma) = (k_0, \gamma_0)$, that

$$t^{-1} \sum_{i \in \mathcal{C}_t} \Lambda_i \sum_{j=1}^{n_i} r_{ij}^{\gamma_0} [\log(r_{ij})]^4 \rightarrow g_4 > 0 \quad (\text{A2.10})$$

in probability as $t \rightarrow \infty$, and that

$$t^{-\frac{1}{2}} E(\sup_{i \in \mathcal{B}_t} |\log(r_{ij_i})|) \rightarrow 0 \quad (\text{A2.11})$$

as $t \rightarrow \infty$. We will not prove these assertions here, but we conjecture that they are satisfied provided the birth-and-death process tends to stabilize as $t \rightarrow \infty$ and that the observation window grows steadily with t . If the whole of S is observed at all times, it seems likely that (A2.7)-(A2.10) follow from an ergodic theorem provided the spatial birth-and-death process tends to stabilize as $t \rightarrow \infty$. This, however, is not the right kind of asymptotics to use for our dune field images. In that situation a growing image size corresponds to observing a larger part of S as well as a longer time interval. Therefore in the dune context, we ought to consider a sequence of birth-and-death processes with $|S|$ increasing proportionally to the observation time t . We still expect (A2.7)-(A2.11) to hold.

The quadratic variation of the vector martingale $(i_k, i_\gamma)^T$ (T denotes transposition) is

$$J_t = \begin{Bmatrix} k_0^{-2} \# \mathcal{B} & k_0^{-1} \sum_{i \in \mathcal{B}_t} \log(r_{ij_i}) \\ k_0^{-1} \sum_{i \in \mathcal{B}_t} \log(r_{ij_i}) & \sum_{i \in \mathcal{B}_t} [\log(r_{ij_i})]^2 \end{Bmatrix}. \quad (\text{A2.12})$$

This matrix is the incremental observed information about k and γ , see Barndorff-Nielsen and Sørensen (1989). The expected information is $i_t = E(J_t)$. Note that the compensators of the entries in J_t are the un-normalized sums in (A2.7)-(A2.9).

A2.6

Under (A2.7)-(A2.10) it follows from the law of large numbers for martingales (Lepingle, 1978) that as $t \rightarrow \infty$

$$t^{-1} J_t \rightarrow G(k_0, \gamma_0) \quad (\text{A2.13})$$

in probability and

$$t^{-1} i_t \rightarrow G(k_0, \gamma_0) \quad (\text{A2.14})$$

From (A2.11), (A2.13) and (A2.14) it follows by a central limit theorem for vector martingales in Hutton and Nelson (1984) that

$$t^{-\frac{1}{2}} (i_k, i_\gamma)^T \rightarrow N(0, G(k_0, \gamma_0)) \quad (\text{A2.15})$$

in distribution as $t \rightarrow \infty$.

The maximum likelihood estimator $\hat{\gamma}_t$ of γ is found by maximizing the profile likelihood $L_3(\gamma)$ given by (4.6). In Section 4 it was proved that $\tilde{l}(\gamma) = \log L_3(\gamma)$ is almost surely strictly concave for all t . The estimator $\hat{\gamma}_t$ can, of course, also be found by maximizing

$$h_t(\gamma) = t^{-1} \{ \tilde{l}_t(\gamma) + \# \mathcal{B}_t \log(t) \} \quad (\text{A2.16})$$

$$= t^{-1} \sum_{i \in \mathcal{B}_t} \gamma \log(r_{ij_i}) - t^{-1} \# \mathcal{B}_t \log \left[t^{-1} \sum_{i \in \mathcal{B}_t} \Delta_i \sum_{j=1}^{n_i} r_{ij}^\gamma \right].$$

It follows from (A2.7)-(A2.9) that

$$h_t(\gamma) \rightarrow \gamma k_0 g_2(\gamma_0) - k_0 g_1(\gamma_0) \log(g_1(\gamma)) = h(\gamma) \quad (\text{A2.17})$$

in probability as $t \rightarrow \infty$ for $\gamma \in \Gamma$. By Theorem II.1 in Andersen and Gill (1982) we conclude that $h(\gamma)$ is concave and that the convergence in (A2.17) is uniform for $\gamma \in K$, where $K \subset \Gamma$ is compact. By standard arguments it follows that $\hat{\gamma}_t \rightarrow \gamma_0$ in probability as $t \rightarrow \infty$.

The maximum likelihood estimator of k satisfies

$$\hat{k}_t = \frac{\#B_t}{\sum_{i \in \mathcal{C}_t} \Lambda_i \sum_{j=0}^{n_i} r_{ij}^{\hat{\gamma}_t}}. \quad (\text{A2.18})$$

To prove that \hat{k}_t is weakly consistent we must verify that the convergence (A2.7) is uniform, for example for γ in a compact set containing γ_0 in its interior. Rewrite (A2.7) in the form

$$t^{-1} \sum_{i \in \mathcal{C}_t} \Lambda_i \sum_{j=1}^{n_i} \left[\frac{r_{ij}}{|S|} \right]^\gamma \rightarrow |S|^{-\gamma} g_1(\gamma), \quad (\text{A2.19})$$

and note that the expression to the left in (A2.19) is convex for all t . Therefore, we can again use Theorem II.1 of Andersen and Gill (1982) to conclude that the convergence in (A2.19) is uniform on all compact subsets of Γ , and hence so is the convergence in (A2.7). Under (A2.7) the law of large numbers for martingales (Lepingle, 1978) implies that $t^{-1} \#B_t \rightarrow k_0 g_1(\gamma_0)$ in probability, so in conclusion $\hat{k}_t \rightarrow k_0$ in probability as $t \rightarrow \infty$. The asymptotic normality of $(\hat{k}_t, \hat{\gamma}_t)$ follows from the usual Taylor expansion of the score function around $(\hat{k}_t, \hat{\gamma}_t)$,

$$t^{-\frac{1}{2}} [\dot{l}_k(k_0, \gamma_0), \dot{l}_\gamma(k_0, \gamma_0)]^T = -t^{-\frac{1}{2}} \ddot{l}_{k\gamma}(\tilde{k}_t, \tilde{\gamma}_t) (\hat{k}_t - k_0, \hat{\gamma}_t - \gamma_0)^T, \quad (A2.20)$$

where $(\tilde{k}_t, \tilde{\gamma}_t)$ is a point between $(\hat{k}_t, \hat{\gamma}_t)$ and (k_0, γ_0) , while

$$\ddot{l}_{k\gamma} = - \left\{ \begin{array}{cc} k^{-2} \# \mathcal{B}_t & \sum_{i \in \mathcal{E}_t} \Delta_i \sum_{j=0}^{n_i} r_{ij}^\gamma \log(r_{ij}) \\ \sum_{i \in \mathcal{E}_t} \Delta_i \sum_{j=0}^{n_i} r_{ij}^\gamma \log(r_{ij}) & k \sum_{i \in \mathcal{E}_t} \Delta_i \sum_{j=0}^{n_i} r_{ij}^\gamma [\log(r_{ij})]^2 \end{array} \right\} \quad (A2.21)$$

is the matrix of second derivatives of the log-likelihood function. The matrix $j_t = -\ddot{l}_{k\gamma}$ is the observed information about (k, γ) . From (A2.7)-(A2.9) it follows that

$$t^{-1} j_t(\tilde{k}_t, \tilde{\gamma}_t) \rightarrow G(k_0, \gamma_0) \quad (A2.22)$$

in probability. Here we have used that also the convergences (A2.8) and (A2.9) are uniform on compact subsets of Γ . This is proved the same way as for (A2.7). We see that the asymptotic covariance matrix of $(\hat{k}_t, \hat{\gamma}_t)$ can be estimated by j_t , i_t or J_t and, of course, by the incremental expected information I_t too. The matrix I_t is the quadratic characteristic of the score martingale.

The asymptotic distributions of the likelihood ratio test statistics also follow by standard techniques. As a brief and

simple reminder of these, note that the likelihood ratio test statistic of the point hypothesis $(k, \gamma) = (\bar{k}, \bar{\gamma})$ can be written in the form

$$2[l(\hat{k}_t, \hat{\gamma}_t) - l(\bar{k}, \bar{\gamma})] = (\hat{k}_t - \bar{k}, \hat{\gamma}_t - \bar{\gamma}) j_t(\tilde{k}_t, \tilde{\gamma}_t) (\hat{k}_t - \bar{k}, \hat{\gamma}_t - \bar{\gamma})^T.$$

Here l is the part of the log-likelihood function related to (k, γ) , and $(\tilde{k}_t, \tilde{\gamma}_t)$ is a point between $(\hat{k}_t, \hat{\gamma}_t)$ and $(\bar{k}, \bar{\gamma})$.

Finally, we shall consider two results used in Section 6. First that (6.4) is asymptotically standard normal. Define $\mathcal{D}_t = \mathcal{D} \cap \mathcal{G}_t$ and the filtration $\mathcal{G}_i = \sigma$ (history of the birth-and-death process in the time interval $[t_0, t_{i-1}]$), $i \in \mathbb{N}$. Since $E(Z_i | \mathcal{G}_i) = 0$ and $E(Z_i^2 | \mathcal{G}_i) = 1$, $i \in \mathbb{N}$, with Z_i given by (6.3), we see that

$$V_i = \sum_{j \in \mathcal{G}_{t_i} \cup \mathcal{D}_{t_i}} Z_j, \quad i \in \mathbb{N},$$

is a zero-mean square integrable discrete time martingale with respect to $\{\mathcal{G}_i\}$, and that the quadratic characteristic of V_i is

$$\langle V \rangle_i = \#(\mathcal{G}_{t_i} \cup \mathcal{D}_{t_i}).$$

The central limit theorem for martingales, see Hall and Heyde (1980), implies asymptotic normality of (6.4) provided the following conditional Lindberg condition holds

$$\langle V \rangle_i^{-1} \sum_{j \in \mathcal{B}_{t_i} \cup \mathcal{D}_{t_i}} E(Z_j^2 | \mathcal{G}_j) \mathbf{1}_{\{|Z_j| > \epsilon N_i^{\frac{1}{2}}\}} \rightarrow 0 \quad (\text{A2.23})$$

in probability as $\langle V \rangle_i \rightarrow \infty$ for all $\epsilon > 0$. Since the fourth conditional moment of Z_j is

$$E(Z_j^4 | \mathcal{G}_j) = p_j^{-1} (1-p_j)^{-1-3},$$

it follows by a Liapounov-type argument that (A2.23) is satisfied if

$$\langle V \rangle_i^{-1} \sum_{j \in \mathcal{B}_{t_i} \cup \mathcal{D}_{t_i}} p_j^{-1} (1-p_j)^{-1} \rightarrow 0 \quad (\text{A2.24})$$

in probability as $\langle V \rangle_i \rightarrow \infty$. One would expect this to be true if the birth-and-death process tends to stabilize.

The second assertion in Section 6 that needs consideration is that $H(x) - F(x)$ tend to zero, where H and F are given by (6.6) and (6.7). The sum

$$W_k = \sum_{j \in \mathcal{B}_{t_k}} [1_{\{r_{ij_i} \leq x\}}^{-F_i(x)}], \quad k \in \mathcal{B},$$

is a zero-mean square integrable discrete time martingale with respect to the filtration $\{\mathcal{F}_k: k \in \mathcal{B}\}$ defined earlier in this appendix. Note that $\mathcal{F}_k = \mathcal{G}_k$ for $k \in \mathcal{B}$. The quadratic characteristic of W is

$$\langle W \rangle_k = \sum_{i \in \mathcal{B}_{t_k}} F_i(x) (1 - F_i(x)) ,$$

so the law of large numbers for martingales, see Lepingle (1978) or Hall and Heyde (1980, p. 35-36), implies that

$$\langle W \rangle_k^{-1} W_k \rightarrow 0$$

almost surely on $\{\langle W \rangle_k \rightarrow \infty\}$. From this $H(x) \doteq F(x)$ follows provided

$$(\#\mathcal{B}_{t_k})^{-1} \langle W \rangle_k = o_p(1) \quad (\text{A2.25})$$

which seems likely to hold if the process stabilizes as $t \rightarrow \infty$. The condition (A2.25) could have been avoided by replacing $\#\mathcal{B}_{t_k}$ by $\langle W \rangle_k$ in the definition of H and F .

References:

Andersen, P.K. and Gill, R.D. (1982): Cox's regression model for counting processes: A large sample study. Ann. Statist. 10, 1100-1120.

Baddeley, A. and Møller, J. (1989): Nearest-neighbour Markov point processes and random sets. Internat. Statist. Rev. 57, 2, 89-121.

Barndorff-Nielsen, O.E. (1978): Information and Exponential Families. Wiley, Chichester.

Barndorff-Nielsen, O.E. and Jørgensen, B. (1990): Some parametric models on the simplex. Research Report No. 199, Department of Theoretical Statistics, Aarhus University.

Barndorff-Nielsen, O.E. and Sørensen, M. (1989): Asymptotic likelihood theory for stochastic processes. A review. Research Report No. 169, Department of Theoretical Statistics, Aarhus University.

Cox, D.R. (1975): Partial likelihood. Biometrika 62, 269-276.

Diggle, P.J. (1983): Statistical Analysis of Spatial Point Patterns. Academic Press, London.

Hall, P.G. and Heyde, C.C. (1980): Martingale Limit Theory and Its Application. Academic Press, New York.

- Holley, R.A. and Stroock, D.W. (1978): Nearest neighbour birth and death processes on the real line. Acta Math., 140, 103-154.
- Hutton, J.E. and Nelson, P.I. (1984): A mixing and stable central limit theorem for continuous time martingales. Technical Report No. 42, Kansas State University.
- Jacobsen, M. (1990): Discrete exponential families: Deciding when the maximum likelihood estimator exists and is unique. Scand. J. Statist. (to appear).
- Lepingle, D. (1978): Sur le comportement asymptotique des martingales locales. In Lecture Notes in Mathematics, 649. Springer, Berlin.
- Møller, J. (1989): On the rate of convergence of spatial birth-and-death processes. Ann. Inst. Statist. Math., 41, 565-581.
- Patefield, W.M. (1977): On the maximized likelihood function. Sankhyā B 39, 92-96.
- Preston, C.J. (1977): Spatial birth-and-death processes. Bull. Int. Statist. Inst. 46 (2), 371-391.
- Richards, F.S.G. (1961): A method of maximum likelihood estimation. J. Roy. Statist. Soc. B 23, 469-475.

Ripley, B.D. (1977): Modelling spatial patterns (with Discussion). J. Roy. Statist. Soc. B 39, 172-212.

Ripley, B.D. (1981): Spatial Statistics. Wiley, New York.

Tsoar, H. and Møller, J.T. (1986): The role of vegetation in formation of linear sand dunes. In W.G. Nickling (ed.): Aeolian Geomorphology, Allen and Unwin, Boston.